EFFICIENT THREE-DIMENSIONAL SURVEY TECHNIQUES AND THEIR COMPARISON IN OPEN SOFTWARE IN THE ARCHAEOLOGICAL TEST SITE OF "NINFEO MAGGIORE" AND "NINFEO MINORE" OF FORMIA (LATINA, ITALY)

L. Alessandri[1], V. Baiocchi[2*], G. Melandri[3], F. Monti[2], A. Canu[4],
L. Ruzzi[5], G. Servodio[4]

[1] Groningen Institute of Archaeology, University of Groningen, Groningen, Netherlands- l.alessandri@rug.nl
[2] Sapienza University of Rome, DICEA, Rome, Italy – (valerio.baiocchi, felicia.monti)@uniroma1.it
[3] Soprintenza archeologica Belle arti e paesaggio per le Provincie di Frosinone e Latina, Italy- gianluca.melandri@beniculturali.it
[4] Microgeo S.r.l., Rome, Italy – (a.canu, g.servodio)@microgeo.it
[5]SITERRA STP S.r.l., Rome, Italy – info@siterra.it

Commission IV, WG IV/4

KEY WORDS: Formia, SLAM, CloudCompare, Ninfeo Maggiore, Villa Romana di Caposele, Ninfeo Minore.

ABSTRACT:

In Europe and beyond, the cultural and archaeological heritage may have considerable extensions of hundreds of square metres if not kilometres. It is then necessary to study highly efficient techniques able , at the same time, to maintain centimetric accuracy. In these contexts, the SLAM technique can be an efficient solution. We tested the latter in a survey of a portion of the so-called Roman Villa of Caposele, also known as Villa Rubino in Formia, (Italy): the "Ninfeo Maggiore" and "Ninfeo Minore" (Major and Minor *nymphaeum*). The two structures had to be surveyed for both conservation and study purposes and to allow a virtual visit, which is particularly important since they are located inside a private property. The structure is complex, with a succession of rooms and environments in an archaeological complex extending approximately 480 metres in an east-west direction and approximately 50 metres in a south-north direction. We decided to survey both *nymphaea* with the "GEOSLAM Zeb Horizon", also surveying all the internal connecting rooms and corridors between them. Both *nymphaea* were also surveyed with a “Faro" terrestrial laser scanning, to allow comparison. To verify the validity of the SLAM on the outside, a survey was carried out using a DJI Matrix drone with laser scanning. The comparison showed very limited deviations whose statistical validation is in progress, demonstrating that the SLAM technique can advantageously be used in such vast archaeological complexes where the efficiency and completeness of the survey is more important than the millimetric accuracy.

1. INTRODUCTION

The geomatic survey of cultural and archaeological heritage is currently at the centre of a fervent debate in the scientific world (Bitelli et al. 2019). The techniques used are very different from the most traditional to the most innovative, from terrestrial photogrammetry (Alessandri et al. 2022; Baiocchi et al. 2017; Del Pizzo et al. 2011) to terrestrial laser scanning (TLS) (Masiero et al. 2019; Angelini et al. 2017, Pirotti et al. 2013) to the numerous studies on the use of UAVs (Pan et al. 2019; Caroti et al. 2015; Lo Brutto et al. 2014). Very often all these techniques, in the case of complex archaeological structures, are used in an integrated manner (Dominici at al. 2013; Ebolese et al. 2019: D’ Agostino et al. 2022; Radicioni et al. 2017). The survey of cultural heritage may require extensive measurement campaigns, especially when the remains extend over large areas and consist of very complex structures. Examples include the complexity and vastness of the Incan cities (Baiocchi et al. 2022), the archaeological deposits in caves (Alessandri et al. 2019) and the quarries and catacombs under the historic cities (Troisi et al. 2107). Surveys must be carried out thoroughly but also efficiently otherwise they become difficult to implement in practice. Without an available detailed survey, it is sometimes impossible to proceed with adeguate restoration after heavy damage or structural failure, as happened in *Pompeii* (Sarhosis et al. 2016) or even in the *Domus Aurea* of the emperor Nero in the centre of Rome (Giavarini, 2001), to name but a few of the best-known examples. Developing and calibrating more or less innovative geomatic techniques to identify the most suitable procedures for surveying large and complex structures in short time, maintaining accuracies of at least the order of a few centimetres has become a priority (Sanz-Ablanedo et al. 2018; Turneret al. 2012; Iheaturu et al. 2020). In the present paper, the SLAM technique was tested in the context of a real archaeological survey on a particularly complex site: the so-called Roman Villa of Caposele, also known as Villa Rubino (Giuliani & Guaitoli, 1972; Cassieri, 2015). The survey has been repeated using more established geomatic techniques to validate the times and geometric correctness characteristics. The Villa, built by the Dukes of Marzano and subsequently passed into the hands of Charles of Ligny, Prince of Caposele, was purchased by King Ferdinando II di Borbone in 1845, to make it a luxurious summer residence. The building overlooks the inlet of Caposele, where there must have been a small harbour, and it is squeezed between the Via Appia and the sea. To the west of the small port are the remains of an imposing structure with a central courtyard, datable to the 1st century B.C., which scholarly tradition has identified as Cicero's Academy or School, although it is probably a *horreum*, testifying to the utilitarian vocation of this area of the villa. In later phases, while retaining its intended use, the *horreum* would be incorporated into a residential building complex together with other structures further to the west that may have served as warehouses in the earlier phase. To the east of the marina is the residential area, the area in which the survey operations were concentrated. Here, on a front about 140 metres long, there are a

* Corresponding author

series of rooms with barrel vaults that were probably part of the *basis villae* of the building. In two of these rooms are the so-called minor and major *nymphaea*. The first consists of an almost quadrangular room with a roof supported by four doric brick columns; on the back wall, in a large niche, spring water gushes out. The wall decorations include stucco, shells and incrustations of glass paste and small stones. The main *nymphaeum* is divided into three naves and covered with a rounded coffered vault supported by doric columns. The large niche at the bottom of the *nymphaeum* contains a pool of spring water; the floor consists of a white mosaic with polychrome *tesserae*. These *nymphaea* constitute the focus of the intervention. In front of them there was a very large fishpond, which ran into the sea for about one hundred metres in length, with a width of over 200m.

The two *nymphaea* surveys had conservative and scientific purposes. One of the aim was to allow a virtual visit, which is particularly important since they are both located inside a private property. As already described, the structure is complex, with a succession of rooms and passageways in an archaeological complex extending approximately 480 metres in an east-west direction and approximately 50 metres in a south-north direction. The survey of such an extension and such an articulation with consolidated techniques such as terrestrial laser scanning would probably have required days, and for this purpose, we wanted to test the possible use of the most modern SLAM techniques, in particular using a GEOSLAM Zeb Horizon, totally transportable by an operator and with a range of up to 100 metres (GEOSLAM, 2022).
The software Cloud Compare 2.11.3 (64 bit) (Cloud Compare DT, 2022) has been used to compare times, modes, precision and accuracy of the point cloud obtained. Cloud Compare allows comparisons and it uses various methods to separately calculating distance and estimating precision and accuracy. It allows one cloud to be fitted to the other or to be compared while remaining within its absolute coordinates.
We decided to survey both *nymphaea* with the "GEOSLAM", also surveying all the internal connecting rooms and passageways between them. The whole survey was carried out in few tens of minutes and afterwards the survey continued over most of the exterior of the entire structure.
The survey of the entire complex was not carried out because the main interest of this project was to test the SLAM technology and validate its precision and accuracy in comparison with more consolidated techniques.
For comparison, both *nymphaea* were surveyed with a more consolidated “Faro" TLS instrument.
To verify the validity of the SLAM also on the external part, a survey was carried out using a DJI Matrix drone with laser scanning. Finally, the same survey was also carried out with an optical camera on the same Matrix drone and with the most widely used drone for photogrammetry, i.e. the "Phantom 4 pro", also by DJI.
All the surveys used the same ground control points, to refer them to the same reference system and to be able to assess their precision and accuracy.
It should be noted that SLAM was only able to station a few of the GCPs while, as can be easily guessed, the drones acquired almost all of them.

2. MATERIALS E METHODS

The instrumentation used in the survey consisted of the DJI Matrice 300 RTK drone to which the DJI P1 optical camera and the DJI L1 LiDAR sensor were attached, the DJI Phantom 4 drone (DJI, 2022), the TLS Faro (Faro, 2022) and the GEOSLAM Zeb Horizon (GEOSLAM, 2022) . The scanning mode of the LiDAR sensor was set to 480 points/m^2. For georeferencing and validation of the accuracy of the different survey types, ground control points were acquired with the E-Survey E300 Pro GNSS system. The photogrammetric reconstruction of the three-dimensional model from the DJI Matrice 300 images (flight with nadiral take and then 45° inclined take) was processed with the DJI Terra 3.4.4 software. The model was georeferenced according to the information obtained in RTK position correction mode, i.e. without the use of GCP. On the other hand, the three-dimensional model obtained from the DJI Phantom 4 images (flight with nadiral take-off) was created with the MicMac v. 1.1 (MicMac DT, 2022) software and oriented with the help of GCPs, achieving an average accuracy of 8.6 cm. This accuracy value was also achieved by correcting the altitude problem often encountered by DJI users. In fact, the 'Absolute Altitude', i.e. the height reported in the EXIF, is often incorrect. It is possible to correct the altitude information of all images.

It should be noted that the complexity of the area analysed by the external surveys of the entire complex (Fig. 1) allowed the acquisition of a small number of points, in a non-ideal conformation. However, all 5 points were used as Ground Control Points (GCPs) to orientate the three-dimensional model of the DJI Phantom 4 and the surveys of the Laser Scanner X and the GEOSLAM Zeb Horizon.

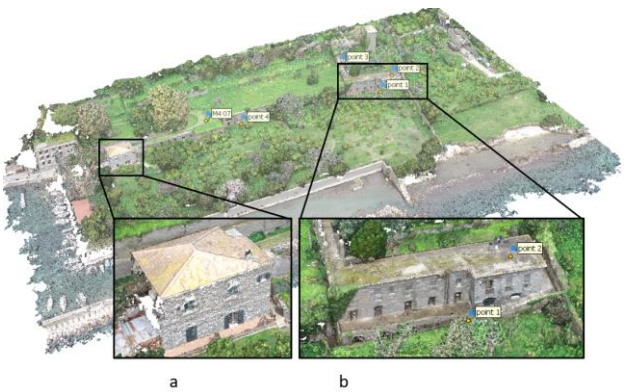

Figure 1. Overall area surveyed outside the complex and distribution of ground control points acquired. The detail boxes show the buildings a) and b) taken into consideration for the comparisons between the various survey methods, presented below.

The variety of instrumentation used for surveying is characterised by different sensors, mounted on different ground and aerial supports, using different positioning modes. Thus, the resulting three-dimensional models are characterised by both the different physical properties of the sensors and the different internal and external orientation parameters. However, we used CloudCompare's Cloud-to-Cloud algorithm (Cloud Compare DT, 2022), which allows us to estimate the distance between two point clouds. Distances are calculated on the cloud identified as 'compared' to the points in the 'reference' cloud. It is good practice to set the densest point cloud as the 'reference' cloud. At the end of the process, a new scalar field is applied to the "compared" cloud containing one scalar field describing the absolute distance and three scalar fields corresponding to the distance calculated along each dimension. In the tests conducted

with the Cloud-to-Cloud tool, the local nearest-neighbour matching model was used, as the tests were performed on the buildings shown in Figure 1, which are characterised by regular surfaces with low roughness. The choice of concentrating the tests on the buildings, rather than on the vegetation present, had the additional purpose of reducing the possibility of contaminating the results of the distances between points with outliers or erroneously highlighting shifts in the elements during the different acquisitions.

Due to the various positioning modes used during the surveys, it was decided to perform further tests with the Cloud-to-Cloud tool after applying Cloud Compare's Fine Registration (ICP) tool. This tool is capable of automatically fine registering two point clouds (or meshes) that have already been roughly registered and represent the same area, i.e. they are overlapping. The 'aligned' point cloud is recorded on the 'reference' cloud according to the set transformation parameters. In fact, shift and rotation with respect to a given axis can be constrained.

3. DISCUSSION

The Cloud-to-Cloud tool was applied to the calculation of the distance between the following point clouds representing the outdoor area:

- DJI Matrice 300 RTK L1/P1

- DJI Phantom 4/DJI Matrice 300 RTK P1

- DJI Matrice 300 RTK L1/DJI Phantom 4

Two sensors were used on the DJI Matrice 300/RTK drone, the DJI P1 optical and the DJI L1 LiDAR. In this case, both clouds obtained were oriented according to the RTK positioning information, without the use of GCPs. The comparison of the two point clouds circumscribed to the building a) depicted in Fig. 1 showed minimal absolute differences, due more to the distance in the z-direction and identified at the areas of discontinuity such as the part below the roof where the window canopies were acquired by LiDAR sensor differently than in the photogrammetric reconstruction (Fig. 2, bottom left and right box).

Distance direction	Gauss mean	St. dev.
	m	m
Absolute distance	0.0476	0.0570
x	0.0040	0.034
y	-0.0049	0.0482
z	-0.0234	0.0375

Table 1. Values obtained after application of the Cloud-to-Cloud tool between DJI Matrice 300 L1 (compared) and P1 (reference) clouds, without the application of Cloud registration.

The comparison of the two three-dimensional models obtained from the optical sensors mounted by the DJI Phantom 4 and the DJI Matrice 300/RTK was carried out by taking element b in Fig. 1 into consideration, as it is in a position that is better modelled by the GCPs than the total external area.

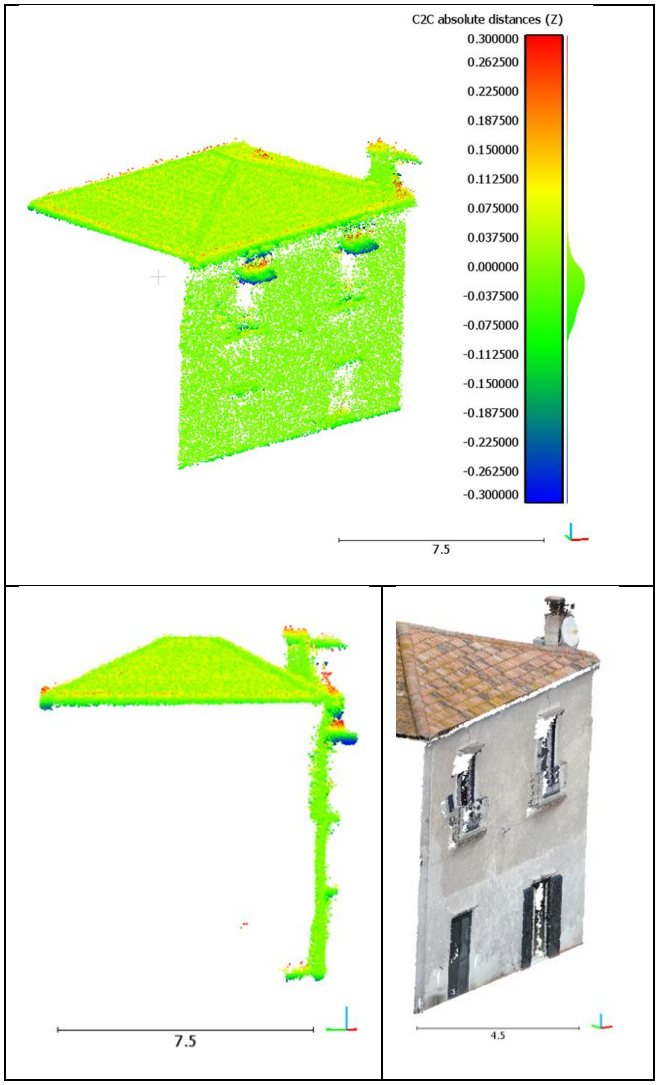

Figure 2. The largest distance values along z calculated are at the window canopies. Below you can see the different acquisition in the case of sensor L1 (left) and P1 (right).

This aspect ensures a lower deformation of the DJI Phantom 4 model, which was oriented on the basis of the GCPs. Also in this case, the greatest distances are detected along the z direction, as can be seen from Fig. 3 on the terrace there is a constant value of approximately 10 cm difference between the two point clouds (green/blue colouration corresponding to the value -0.1 m, negative as the point difference is calculated considering "compared" - "reference" altitude). In particular, the three-dimensional model of the DJI Matrice 300 RTK P1 has higher altitudes than the DJI Phantom 4, this difference could result from errors on the determination of the phase centre of the GPS/RTK antenna or the centre of the sensor acquisition. In this case, a post-registration comparison between the two point clouds was also performed with the 'Clouds registration' tool to highlight any differences between the geometries of the two clouds, disregarding positioning errors. Registration with constrained rotation around the z axis and shift along x,y, z returned no changes on the registered cloud. On the contrary, after applying registration with the possibility of rotation and shift along the three axes, the calculated distances are significantly smaller in all directions (Table 3). Thus, geometrically the clouds are congruent, despite the fact that the DJI Matrice works in RTK, thus, has a more robust frame block

than the Phantom 4 which has lower optical quality but relies on GCPs.

Distance direction	Gauss mean	St. dev.
	m	m
Absolute distance	0.0815	0.0673
x	0.0057	0.0489
y	-0.0110	0.0496
z	-0.0464	0.0633

Table 2. Values obtained after the application of the Cloud-to-Cloud tool between DJI Phantom 4 clouds (compared) and DJI Matrice 300 RTK P1 (reference), without the application of Cloud registration.

Distance direction	Gauss mean	St. dev.
	m	m
Absolute distance	0.0342	0.0675
x	0.0001	0.0465
y	-0.00004	0.0426
z	0.0002	0.0419

Table 3. Values obtained after application of the Cloud-to-Cloud tool between DJI Phantom 4 clouds (compared) and DJI Matrice 300 RTK P1 (reference), after application of Cloud registration (shift and rotation with respect to X, Y, Z).

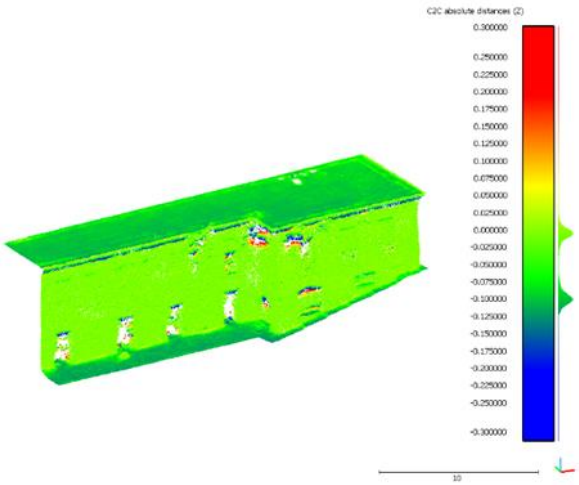

Figure 3. Distances along the z axis resulting from the Cloud-to-Cloud application without registration of the two clouds.

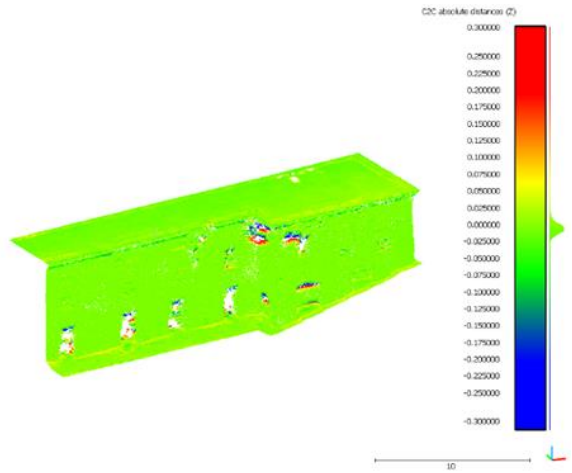

Figure 4. Distances along the z axis resulting from the Cloud-to-Cloud application after registration the two point clouds by setting shift and rotation in the three directions x,y,z.

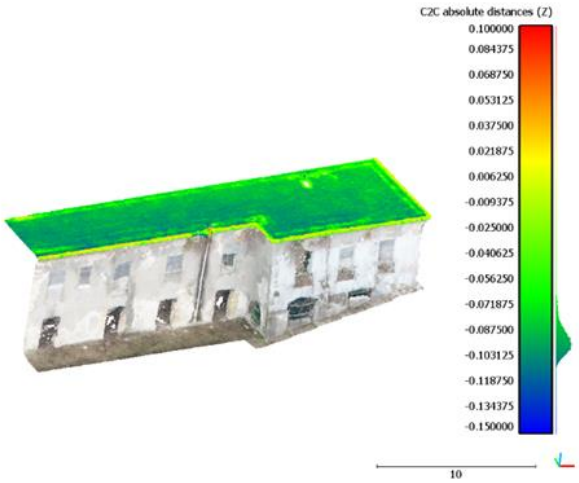

Figure 5. Distances along the z axis resulting from the Cloud-to-Cloud application, without registration of the two clouds.

Figure 6. Distances along the Z axis resulting from the Cloud-to-Cloud application, after registration the two point clouds by setting shift in the three directions x,y,z and rotation with respect to the z axis.

To further test the registration with x,y,z shift and constrained rotation around the z axis, only the portion of the point cloud representing the terrace of building b) was taken into account (Fig. 1). In this case, the tool returned a better geometric congruence between the two point clouds.
Finally, with regard to the external models, the distance between the point clouds acquired by the DJI Matrice 300 RTK L1 and the DJI Phntom 4 was calculated. Note that, similarly to the first comparison, on the terrace there is a constant value of approximately 10 cm difference between the two point clouds (this time the difference in altitude is positive as it is calculated considering "compared" - "reference" altitude, the "compared" altitude is higher). Considering the similar working mode of position correction in RTK of the DJI Matrice 300 RTK drone, this difference could also result from errors in the determination of the phase centre of the GPS/RTK antenna or from the acquisition centre of the sensor.

Distance direction	Gauss mean	St. dev.
	m	m
Absolute distance	0.1009	0.1087
x	-0.0071	0.0542
y	0.0011	0.0593
z	0.0801	0.0951

Table 4. Values obtained after applying the Cloud-to-Cloud tool between DJI Matrice 300 RTK L1 (compared) and DJI Phantom 4 (reference) clouds, without Cloud registration.

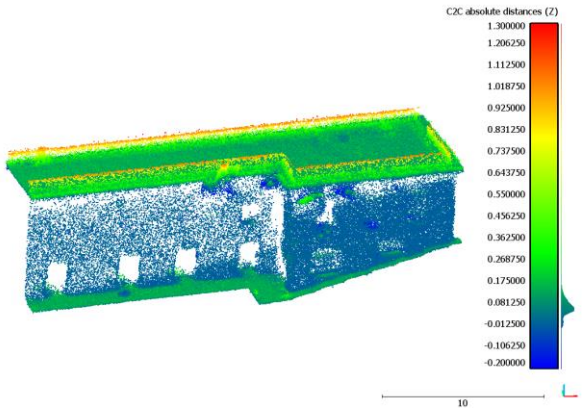

Figure 7. Distances along the z-axis resulting from the Cloud-to-Cloud application, the registration of the two point clouds was not applied.

The internal surveys of the Major Nymphaeum and the Minor Nymphaeum were carried out with the TLS Faro and the GEOSLAM Zeb Horizon. The entire environment was acquired with several stations with the TLS, but having worked in the absence of spherical markers, it was decided to use a single acuisition that was more representative of the actual geometry of the site, in order to perform comparisons on a robust point cloud. The scheme followed for calculating the distance between the point clouds representing the interior areas follows that used for the exterior. Thus, only comparisons were made between the original point clouds and tr recorded point clouds (with shift in x,y,z and rotation around z and then around x,y,z). The superposition of the original TLS and GEOSLAM point clouds representing the Nymphaeum Major shows an obvious shift. However, the cloud registration tool does not improve the superposition of the data, probably due to their complex three-dimensional structure (Fig. 8 a,b,c).
Then the geoslam was recorded on the laser cloud, with shifts in x,y,z, but rotation only on z (Fig. 10)

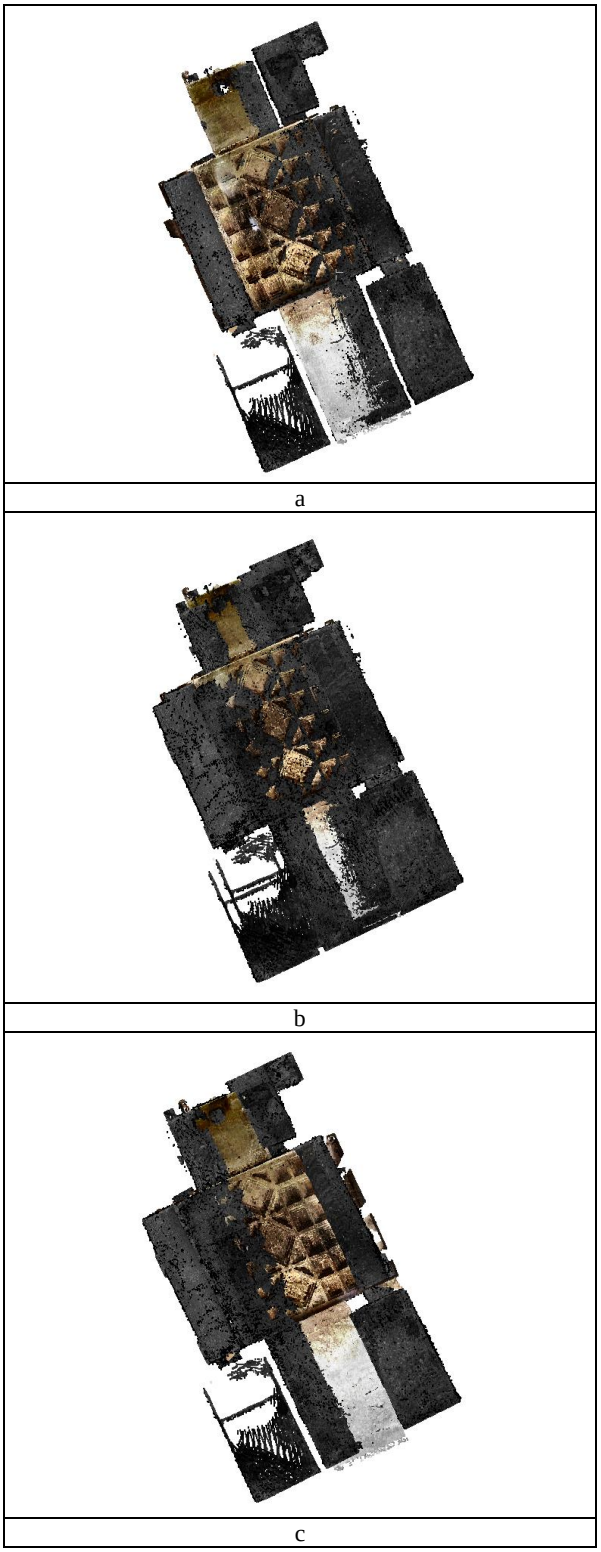

Figure 8. Cloud comparisons from Geoslam and TLS without registration (a), with registration with rotation along the z axis only (b) and with registration with rotation along the three axes x,y,z

The same registration was then tested with shifts in x,y,z and rotations in the three axes (fig. 11)

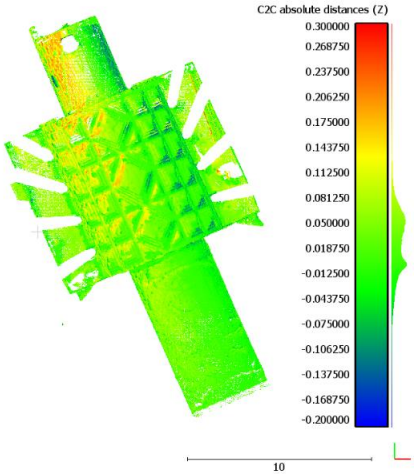

Figure 9. Distances along the z-axis resulting from the Cloud-to-Cloud application, the registration of the two point clouds was not applied.

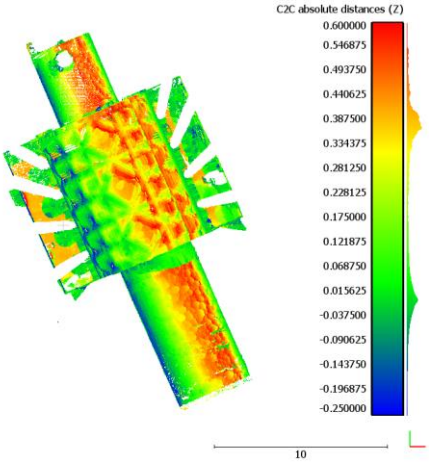

Figure 10. Distances along the Z axis resulting from the Cloud-to-Cloud application, registration was applied (by setting shift in the three directions x, y, z and rotation with respect to the z axis) of the two point clouds.

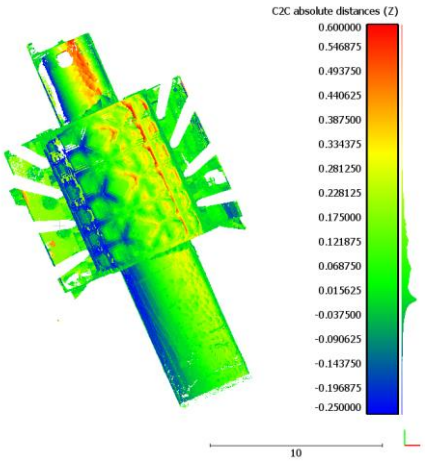

Figure 11. Distances along the z axis resulting from the Cloud-to-Cloud application, registration was applied by setting shift in the three directions x, y, z and rotation with respect to the z axis only.

a

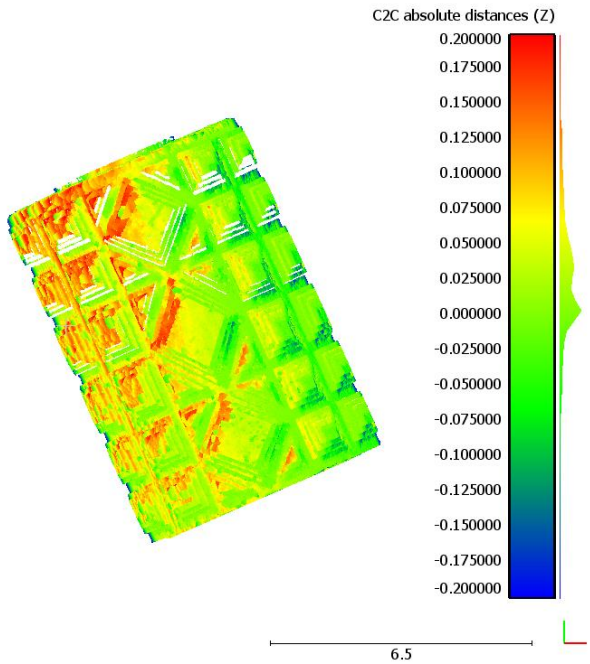

b

Figure 12. Registration of the top part (a) and its distances (b) along the z axis resulting from the Cloud-to-Cloud application, registration was applied (by setting shift in the three directions x, y, z and rotation with respect to the z axis) of the two point clouds.

a

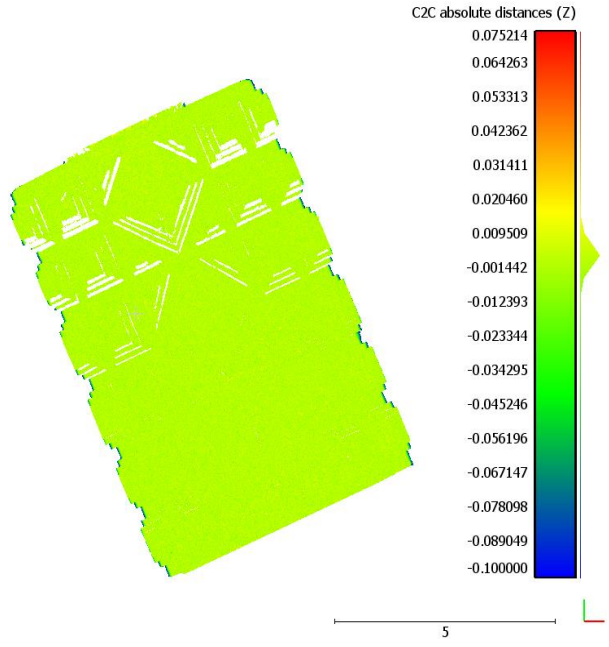

b

Figure 13. Registration of the top part (a) and its distances (b) along the z axis resulting from the Cloud-to-Cloud application, the registration of the two point clouds was applied (setting shift and rotation in the three directions x, y, z.

The same registration of the geoslam cloud on the laser was then performed, with shift along the x,y,z axes and rotation along all three x,y,z axes (fig. 13 a and b)

4. CONCLUSIONS

The present work made it possible to make some initial comparisons in a real archaeological survey operation. With regard to the survey of the internal parts, the possibility of surveying complex structures with Geoslam-type instrumentation was tested in comparison with more classic but costly and time consuming TLS surveys. In particular, it was verified that the survey of the entire internal structure and a large part of the external façade was carried out in less than 20 minutes, while the same survey of the internal parts alone with TLS took more than two hours. Assuming that the TLS is in any case more consistent in terms of maintaining the geometries (for the comparison, data obtained from a single TLS station were used), it would seem that Geoslam holds a good centimetric agreement for the first ten metres of the survey, subsequently increasing its "drift" as was to be expected. This effect would not seem to depend on incorrect georeferencing because even when calibrating one cloud over the other, the results do not seem to worsen. The Geoslam therefore proves to be a very interesting alternative for this type of survey where a large extension must be surveyed even without the accuracy of the more onerous (in terms of time) TLS. However, it is always possible to set up a network of reference points on the route, even in the interior with a classic terrestrial survey using a total station. As far as external clouds are concerned, the survey with RTK drone without ground reference points seems to give results very close to the more traditional use of the drone without RTK but with ground reference points of the GCPs application. The LIDAR survey from the same drone also seems very accurate. Only a systematism in altitude was observed between the RTK clouds and the other surveys all reverted to ground points, which could be due to the imperfect configuration of the height of the antennas on one of the GPS/GNSS receivers or to the use of different GNSS permanent stations and their materialisation. Further experimentation will be aimed at investigating these aspects more thoroughly with specific surveys.

REFERENCES

Alessandri, L., Baiocchi, V., Del Pizzo, S., Di Ciaccio, F., Onori, M., Rolfo, M.F. & Troisi, S., 2022: A flexible and swift approach for 3D image–based survey in a cave, *Applied Geomatics*, vol. 14, 5-19. https://doi.org/10.1007/s12518-020-00309-4

Alessandri, L., Baiocchi, V., Del Pizzo, S., Rolfo, M.F., Troisi, S., 2019: Photogrammetric survey with fisheye lens for the characterization of the la sassa cave, *ISPRS Annals of the Photogrammetry, Remote Sensing and Spatial Information Sciences*, 25. https://doi.org/10.5194/isprs-archives-XLII-2-W9-25-2019

Angelini, M. G., Baiocchi, V., Costantino, D., and Garzia, F., 2017: Scan to BIM for 3d reconstruction of the papal basilica of Saint Francis in Assisi in Italy. *Int. Arch. Photogramm. Remote Sens. Spatial Inf. Sci.*, XLII-5/W1, 47-54, DOI: 10.5194/isprsarchives-XLII-5-W1-47-2017.

Baiocchi, V., Giammarresi, V., Ialongo, R., Piccaro, C., Allegra, M. & Dominici, D., 2017: The survey of the basilica di collemaggio in L'Aquila with a system of terrestrial imaging and most proven techniques, *European Journal of Remote Sensing*, vol. 50, no. 1, 237-253. https://doi.org/10.1080/22797254.2017.1316523

Baiocchi, V., Pizzo, S.D., Monti, F., Pugliano, G., Onori, M., Robustelli, U., Troisi, S., Vatore, F. & Trujillo, F.J.L., 2022: Solutions and limitations of the geomatic survey of an archaeological site in hard to access areas with a latest generation smartphone: the example of the Intihuatana stone in Machu Picchu (Peru), *Acta IMEKO*, vol. 11, no. 1. https://doi.org/10.21014/acta_imeko.v11i1.1117

Bitelli, G., Balletti, C., Brumana, R., Barazzetti, L., D'Urso, M.G., Rinaudo, F., Tucci, G., 2019: The gamher research project for metric documentation of cultural heritage: Current developments", *ISPRS Annals of the Photogrammetry, Remote Sensing and Spatial Information Sciences*, 239.

Caroti, G., Martinez-Espejo Zaragoza, I., Piemonte, A., 2015. Accuracy assessment in structure from motion 3D reconstruction from UAV-born images: The influence of the data processing methods. *Int. Arch. Photogramm. Remote Sens. Spat. Inf. Sci.*, XL-1/W4, 103–109. https://doi.org/10.5194/isprsarchives-XL-1-W4-103-2015.

Cassieri, N., 2015. Nuovi Risultati Di Indagine Dalle Ville Costiere Formiane. *Newsletter Di Archeologia* CISA 6: 67–93.

Cloudcompare development team, 2022, https://www.cloudcompare.org/ (last seen online: 10/06/2022)

D'Agostino, G., Figuera, M., Russo, G., Galizia, M., Militello, P.M., 2022: Integrated 3d survey for the documentation and visualization of a rock-cut underground built heritage, International Archives of the Photogrammetry, Remote Sensing and Spatial Information Sciences - ISPRS Archives, pp. 167.10.5194/isprs-archives-XLVI-2-W1-2022-167-2022

Del Pizzo, S., Troisi, S., 2011: Automatic orientation of image sequences in cultural heritage. *Int. Archives of Photogrammetry, Remote Sensing and Spatial Information Sciences*, 38(5/W16). https://doi.org/10.5194/isprsarchives-XXXVIII-5-W16-293-2011

DJI, 2022, http://www.dji.com (last seen online: 10/06/2022)

Dominici D., Rosciano E., Alicandro M., Elaiopoulos M., Trigliozzi S. and Massimi V., 2013. Cultural heritage documentation using geomatic techniques: Case study: San Basilio's monastery, L'Aquila, *Digital Heritage International Congress (DigitalHeritage)*, Marseille, 2013, 211-214. doi: 10.1109/DigitalHeritage.2013.6743735

Ebolese, D., Lo Brutto, M., Dardanelli, G., 2019: The integrated 3D survey for underground archeological environment. Int. Arch. Photogramm. Remote Sens. Spatial Inf. Sci., XLII-2/W9, 311– 317. doi.org/10.5194/isprs-archives-XLII-2-W9-311-2019.

Faro, 2002, https://www.faro.com/ (last seen online: 10/06/2022)

GEOSLAM, 2022, https://geoslam.com/solutions/zeb-horizon/ (last seen online: 10/06/2022)

Giavarini, C., 2001: Domus Aurea: The conservation project. *Journal of Cultural Heritage*, vol. 2, no. 3, 217-228. https://doi.org/10.1016/S1296-2074(01)01122-0

Giuliani, M., Cairoli, F., Guaitoli, M., 1972: Il Ninfeo Minore Della Villa Detta Di Cicerone a Formia. *Römische Mitteilungen*, 191–219. https://doi.org/10.1007/s10518-016-9881-z

Iheaturu, C., Ayodele, E., Okolie, C., 2020. An Assessment of the accuracy of Structure-from-Motion (SfM) Photogrammetry for 3D terrain mapping. *Geomatics, Landmanagement and Landscape*, 2, 65-82. http://dx.doi.org/10.15576/GLL/2020.2.65.

Lo Brutto, M., Garraffa, A., and Meli, P., 2014: UAV platforms for cultural heritage survey: first results. *ISPRS Ann. Photogramm. Remote Sens. Spatial Inf. Sci*., Vol. II-5, 227-234. https://doi.org/10.5194/isprsannals-II-5-227-2014.

Masiero, A., Chiabrando, F., Lingua, A.M., Marino, B.G., Fissore, F., Guarnieri, A., Vettore, A., 2019: 3d modeling of Girifalco fortress. *Int. Arch. Photogramm. Remote Sens. Spatial Inf. Sci*., XLII-2/W9, 473–478. https://doi.org/10.5194/isprsarchives-XLII-2-W9-473-2019.

MicMac Developer Team, 2022, https://micmac.ensg.eu/index.php/Install_MicMac_Windows (last seen online: 10/06/2022)

Pan, Y., Dong, Y., Wang, D., Chen, A., Ye, Z., 2019: ThreeDimensional Reconstruction of Structural Surface Model of Heritage Bridges Using UAV-Based Photogrammetric Point Clouds. *Remote Sens*., 11, 1204. https://doi.org/10.3390/rs11101204.

Pirotti, F., Guarnieri, A., Vettore, A., 2013: State of the Art of Ground and Aerial Laser Scanning Technologies for High Resolution Topography of the Earth Surface. In *European Journal of Remote Sensing*, n. 46, 66-78.

Radicioni F., Matracchi P., Brigante R., Brozzi A., Cecconi M., Stoppini A., Tosi G., 2017: The Tempio della Consolazione in Todi: integrated geomatic techniques for a monument description including structural damage evolution in time. ISPRS - *Int. Arch. Photogramm. Remote Sens. Spat. Inf. Sci.*, XLII-5/W1, 433-440., https://doi.org/10.5194/isprs-archives-XLII-5-W1-433-2017

Sanz-Ablanedo, E., Chandler, J.H., Rodríguez-Pérez, J.R., Ordóñez, C., 2018. Accuracy of Unmanned Aerial Vehicle (UAV) and SfM Photogrammetry Survey as a Function of the Number and Location of Ground Control Points Used. *Remote Sens.*, 10, 1606. https://doi.org/10.3390/rs10101606.

Sarhosis, V., Asteris, P., Wang, T., Hu, W., Han, Y., 2016: On the stability of colonnade structural systems under static and dynamic loading conditions, *Bulletin of Earthquake Engineering*, vol. 14, no. 4, 1131-1152.

Troisi, S., Baiocchi, V., Del Pizzo, S., Giannone, F., 2017: A prompt methodology to georeference complex hypogea environments. *Int. Arch. Photogramm. Remote Sens. Spatial Inf. Sci.*, XLII-2/W3, 639–644. https://doi.org/10.5194/isprsarchives-XLII-2-W3-639-2017.

Turner, D., Lucieer, A., Watson, C., 2012. An Automated Technique for Generating Georectified Mosaics from UltraHigh Resolution Unmanned Aerial Vehicle (UAV) Imagery, Based on Structure from Motion (SfM) Point Clouds. *Remote Sens*., 4, 1392-1410. https://doi.org/10.3390/rs4051392.